4-2 Optical Heterodyne Detection for 60-GHz-Band Radio-on-Fiber Systems

Toshiaki KURI and Ken-ichi KITAYAMA

A novel method for optical heterodyne detection in millimeter-wave-band radio-on-fiber systems is described. The key to detection is to use a remote dual-mode local light. Although the light is free-running, our method is in principle free from laser phase noise. This method is also theoretically immune from the fiber-dispersion effect, because only two components of the optical signal are selected out by the local light to demodulate themselves. This immunity persists even if the transmitted optical signal is in the double-sideband format. We derive the theoretical limit of the system performance and experimentally demonstrate a 25-km-long fiber-optic transmission and the optical heterodyne detection of a 59.6-GHz radio-on-fiber signal using 155.52-Mb/s DPSK-formatted data.

Keywords
Optical heterodyne detection, Dual-mode local light, Radio-on-fiber, Optical fiber dispersion, Laser phase noise

1 Introduction

External modulation will provide the best solution to configure simpler base stations (BSs) in future microwave or millimeter-wave (mm-wave) radio-on-fober systems, leading to cost-effective system configuration[1]. We have reported on radio-on-fiber systems that use a 60-GHz-band electroabsorption modulator (EAM) for downlinking and uplinking[2][3]. To receive optical power large enough to get high transmission quality, using some optical amplifiers is necessary in the optical link. However, accumulated amplified-spontaneous-emission (ASE) noise from the optical amplifiers cannot be removed completely, in analog optical communication systems, such as radio-on-fiber applications. The noise fatally affects the photodetected signal, resulting in a degradation in system performance. The theory that optical coherent detection using a remote local light source has higher-sensitivity to a received optical signal than direct detection under a shot-noise-limited condition is well known[4]. Thus, we expect that if we use the coherent detection technique, we can avoid using optical amplifiers. Laser phase noise and polarization mismatch cause this degradation if we consider using a remote local light source for optical heterodyne detection. Because the polarization mismatch is a common problem for optical fiber systems, we concentrate on using optical heterodyne detection that is insensitive to laser phase noise.

In this paper, we describe a novel method for optical heterodyne detection in radio-on-fiber systems at a 60-GHz band. A free-running dual-mode local light is used to detect a 60-GHz-band radio-on-fiber signal. We show that the system, in principle, is not affected by the phase noises not only for the transmitting laser but also for the remote local one. This scheme is also theoretically immune from the fiber-dispersion effect which causes signal fading, because only two components of the optical signal are selected out by the local light to demodulate themselves. This immunity persists even if the transmitted optical signal is in a double-sideband (DSB) format.

Although some dispersion-free systems[5][6] have been proposed, they have never essentially solved the ASE problem. We present a principle together with a mathematical description of signals in our method and derive the theoretical limit of the system performance. We experimentally verify the principle of our method by demonstrating a 25-km-long fiber-optic transmission and the optical heterodyne detection of a 59.6-GHz radio-on-fiber signal using 155.52-Mb/s differential-phase-shift-keying (DPSK).

2 Principle

2.1 Mathematical Description

Fig.1 shows the fundamental block diagram of the optical heterodyne detection using dual-mode local light source. The transmitter consists of a single-mode light source and optical external and electrical modulators. Also, the optical heterodyne receiver consists of a dual-mode local light source, optical power combiner, photodetector (PD), phase noise canceling (PNC) circuit, and electrical demodulator.

The complex electric field of the optical carrier, $e_{c1}(t)$, which is oscillated from the single-mode light source in the transmitter, is written as

$$e_{c1}(t) = E_{c1} \cdot \exp\{j\varphi_{c1}(t)\}, \quad (1)$$
$$\varphi_{c1}(t) = 2\pi f_{c1} t + \phi_{c1}(t), \quad (2)$$

where E_{c1}, f_{c1}, and $\phi_{c1}(t)$ are the amplitude, the center frequency, and the phase noise of the optical carrier, respectively. The radio-frequency (RF) signal, $e_{RF}(t)$, is written as

$$e_{RF}(t) = V_{RF} \cdot \exp\{j\varphi_{RF}(t)\}, \quad (3)$$
$$\varphi_{RF}(t) = 2\pi f_{RF} t + \theta(t), \quad (4)$$

where V_{RF}, f_{RF}, and $\theta(t)$ represent the amplitude, the carrier frequency, and the phase-modulated data of the RF signal, respectively. The optical carrier, $e_{c1}(t)$, is modulated by the RF signal, $e_{RF}(t)$, and transmitted over the optical fiber. Taking into account the fiber-dispersion effect, after the propagation in the optical fiber of the length, L, the complex electric field of the modulated optical signal is generally written as

$$\begin{aligned} e_s(t,L) &= \mathrm{MOD}[e_{RF}(t)] \cdot e_{c1}(t) \cdot e^{-j\beta(f)\cdot L} \\ &= E_{c1} \cdot \sum_{n=-\infty}^{\infty} a_n \cdot e^{j\varphi_{s,n}(t,L)}, \quad (5) \\ \varphi_{s,n}(t,L) &= \varphi_{c1}(t) + n\varphi_{RF}(t) - \beta(f)\cdot L \\ &\simeq 2\pi(f_{c1} + nf_{RF})(t - \beta_1 L) \\ &\quad + n\theta(t - \beta_1 L) + \phi_{c1}(t - \beta_1 L) \\ &\quad - \frac{1}{2}\beta_2 (2\pi n f_{RF})^2 \cdot L \\ &\quad + (2\pi f_{c1}\cdot\beta_1 - \beta_0)\cdot L. \quad (6) \end{aligned}$$

Here, $\beta(f)$ is the propagation constant and is approximated as[7]

$$\beta(f) = \sum_{i=0}^{\infty} \frac{\beta_i}{i!} \{2\pi(f - f_{c1})\}^i \quad (7)$$

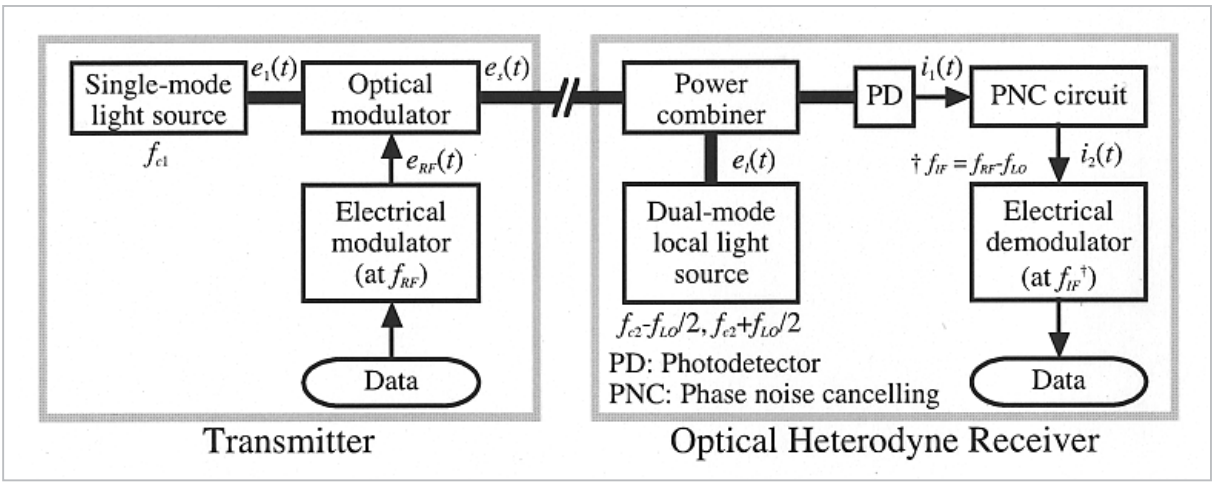

Fig.1 *Block diagram of proposed optical heterodyne detection schme*

$$\simeq \beta_0 + \beta_1 2\pi (f - f_{c1}) + \frac{1}{2}\beta_2 \{2\pi (f - f_{c1})\}^2, \quad (8)$$

where $\beta_1 L$ corresponds to the group delay time and β_2 is related with the dispersion, D, as

$$\beta_2 = -\frac{\lambda^2}{2\pi c} \cdot D. \quad (9)$$

λ and c are the wavelength in the fiber and the velocity in the vacuum, respectively. Note that the last term in Eq.(6) is constant and independent of time and the last second term represents the chromatic fiber-dispersion effect. Then, MOD[•] represents the response function of the optical modulator, depending on the scheme used in the modulator, such as intensity, phase, or frequency. Therefore, a_n is given as the Fourier coeffcient of MOD[•]. If the intensity modulation is performed and the modulation index, m_{IF}, is small, for example, then the Fourier coeffcients are written approximately as[8]

$$a_0 \simeq \sqrt{\frac{1}{2}}\left[1 - \left(\frac{m_{IM}}{4}\right)^2\right], \quad (10)$$

$$a_{\pm n} \simeq (-1)^{n-1}\sqrt{\frac{1}{2}}\frac{(2n-3)!!}{n!}\left(\frac{m_{IM}}{4}\right)^n \quad \text{for } n \neq 0, \quad (11)$$

where $(2n+1)!! \equiv 1 \cdot 3 \cdots (2n+1)$, $(2n)!! \equiv 2 \cdot 4 \cdots (2n)$, and $0!! \equiv (-1)!! \equiv 1$. The details are described in Appendix A[8]. If the input amplitude of the modulating signal is small ($V_{RF} \ll 1$), then $e_s(t)$ is approximated as

$$e_s(t, L) \simeq E_{c1} \cdot a_{-1} \cdot e^{j\varphi_{s,-1}(t,L)} + E_{c1} \cdot a_0 \cdot e^{j\varphi_{s,0}(t,L)} + E_{c1} \cdot a_1 \cdot e^{j\varphi_{s,1}(t,L)}. \quad (12)$$

The free-running dual-mode local light that has a frequency separation of f_{LO} is used to detect the radio-on-fiber signal, $e_s(t, L)$, in the optical heterodyne receiver. Here, the dual-mode light source is considered to have a frequency separation that is either highly stabilized or jitter-free. The complex electric field of the dual-mode local light, $e_l(t)$, is written as

$$e_l(t) = \sqrt{\frac{1}{2}}E_{c2} \cdot \exp\{j\varphi_{l-}(t)\} + \sqrt{\frac{1}{2}}E_{c2} \cdot \exp\{j\varphi_{l+}(t)\}, \quad (13)$$

$$\varphi_{l-}(t) = 2\pi\left(f_{c2} - \frac{f_{LO}}{2}\right)t + \phi_{c2}(t), \quad (14)$$

$$\varphi_{l+}(t) = 2\pi\left(f_{c2} + \frac{f_{LO}}{2}\right)t + \phi_{c2}(t), \quad (15)$$

where E_{c2}, f_{c2}, and $\Phi_{c2}(t)$ are the amplitude, the center frequency, and the phase noise of the dual-mode local light, respectively. The dual-mode local light, $e_l(t)$, is combined with the received optical signal, $e_s(t, L)$, as shown in Fig.2. The optical heterodyne detection is performed using a square-law response of the PD. Let us assume that the polarizations between the received optical signal and the local light are matched. Then, the photocurrent becomes

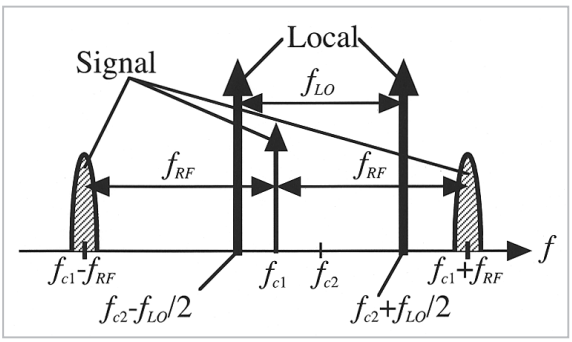

Fig.2 *Optical spectra of signal $e_s(t)$ and local $e_l(t)$*

$$(t) = \mathcal{R}\sqrt{2P_{c1}P_{c2}}a_0 e^{j(\varphi_{s,0}(t,L)-\varphi_{l-}(t))} + \mathcal{R}\sqrt{2P_{c1}P_{c2}}a_1 e^{j(\varphi_{s,1}(t,L)-\varphi_{l+}(t))} + \mathcal{R}\sqrt{2P_{c1}P_{c2}}a_0 e^{j(\varphi_{l+}(t)-\varphi_{s,0}(t,L))} + \mathcal{R}\sqrt{2P_{c1}P_{c2}}a_{-1} e^{j(\varphi_{l-}(t)-\varphi_{s,-1}(t,L))} + \cdots. \quad (16)$$

In the above equation, P_{c1} and P_{c2} are the photodetected power of the signal and local light, respectively and are given as[9]

$$P_{c1} = \int_A \frac{|e_{c1}(t)|^2}{2Z_w}dA, \quad (17)$$

$$P_{c2} = \int_A \frac{|e_{c2}(t)|^2}{2Z_w}dA. \quad (18)$$

Here, A and Z_w represent the photodetecting effective area and the wave impedance, respectively. Note that $\mathcal{R}$ is the responsivity of the PD. We focus on the two phase compo-

nents:

$$\begin{aligned}
&\varphi_{s,0}(t,L)-\varphi_{l-}(t)\\
&= 2\pi\left(\Delta f+\frac{f_{LO}}{2}\right)(t-\beta_1 L)\\
&\quad +\Delta\phi_c(t,L)\\
&\quad +\left\{2\pi\left(\Delta f+\frac{f_{LO}}{2}\right)\beta_1-\beta_0\right\}\cdot L, \qquad (19)\\
&\varphi_{s,1}(t,L)-\varphi_{l+}(t)\\
&= 2\pi\left(\Delta f+f_{RF}-\frac{f_{LO}}{2}\right)(t-\beta_1 L)\\
&\quad +\theta(t-\beta_1 L)+\Delta\phi_c(t,L)\\
&\quad -\frac{1}{2}\beta_2(2\pi f_{RF})^2\cdot L\\
&\quad +\left\{2\pi\left(\Delta f+f_{RF}-\frac{f_{LO}}{2}\right)\beta_1\right.\\
&\quad \left.-\beta_0\right\}\cdot L, \qquad (20)
\end{aligned}$$

where Δf and $\Delta\phi_c(t, L)$ are defined as

$$\begin{aligned}
\Delta f &\equiv f_{c1}-f_{c2}, \qquad (21)\\
\Delta\phi_c(t,L) &\equiv \phi_{c1}(t-\beta_1 L)-\phi_{c2}(t). \qquad (22)
\end{aligned}$$

There are two possible configurations for the PNC, (a) using an electrical square-law detector (PNC_1) and (b) using an electrical multiplier (PNC_2)[10], as shown in Fig.3. In Fig.3 (a), BPF_{11} in PNC_1 filters out two components of $\Delta f+f_{LO}/2$ and $\Delta f+f_{RF}-f_{LO}/2$ simultaneously. They are squared by PNC_1. Then, only the down-converted signal at f_{IF} [$\equiv f_{RF}-f_{LO}$], $i_2(t)$, is filtered out by BPF_{12}.

$$\begin{aligned}
i_2(t) &\propto \frac{1}{2}\mathcal{R}^2 P_{c1}P_{c2}a_0a_1e^{j\varphi_{IF}(t,L)} \qquad (23)\\
\varphi_{IF}(t,L) &= \{\varphi_{s,1}(t,L)-\varphi_{l+}(t)\}\\
&\quad -\{\varphi_{s,0}(t,L)-\varphi_{l-}(t)\}\\
&= 2\pi f_{IF}(t-\beta_1 L)+\theta(t-\beta_1 L)\\
&\quad -\{\beta_0-2\pi f_{IF}\beta_1\\
&\quad +\frac{1}{2}\beta_2(2\pi f_{RF})^2\Big\}\cdot L \qquad (24)
\end{aligned}$$

In PNC_2, two components of $\Delta f+f_{LO}/2$ and $\Delta f+f_{RF}-f_{LO}/2$ are filtered out each by BPF_{21} and BPF_{22}, respectively, as shown in Fig.3 (b). They multiply each other, and only the down-converted signal at f_{IF} , $i_2(t)$, is filtered out by BPF_{23}, which is identical to BPF_{12}. Also, in this case, $i_2(t)$ becomes the same signal expressed in Eq. (23), except that the amplitude becomes half. The difference of PNC_1 and PNC_2 is the amount of the noise put into the square-law detector or the multiplier because of the difference in the bandwidths of

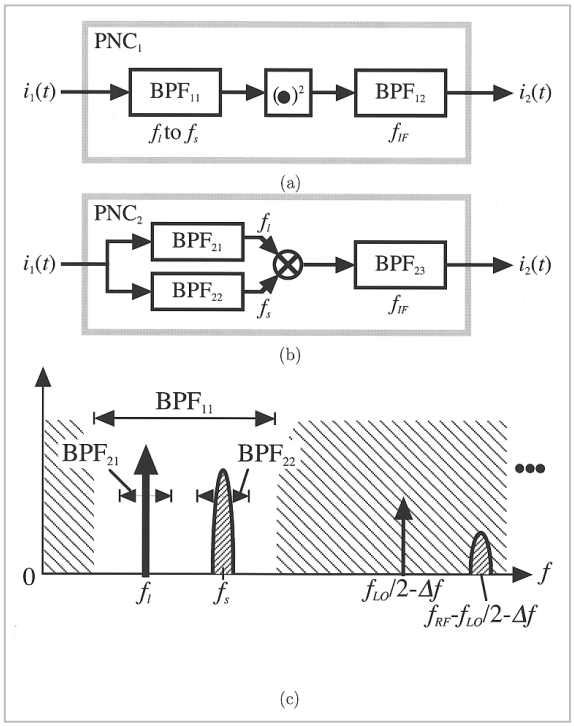

Fig.3 *PNCs (a) with square-law detector (PNC_1) and (b) with multiplier (PNC_2). (c) Photodetected signals and pass-bands of BPF_{11}, BPF_{21}, and BPF_{22}*

BPF_{11}, BPF_{21}, and BPF_{22}, as shown in Fig.3 (c). This will cause an absolute amount of noise because of a *noise*×*noise* term included in PNC_1 output that is larger than PNC_2 output. However, the *noise*×*noise* term is usually negligible for practical use, in which the signalto-noise power ratio (SNR) is relatively high so that data can be transmitted with high quality. Therefore, the system performances for the systems using PNC_1 and PNC_2 will be almost the same.

Based on the above theoretical description, we can describe the features. First, the absence of laser phase-noise remains in Eqs. (23) and (24). This means that our method is in principle free from the laser phase noise. Second, the last term in Eq. (24) represents the phase delay for the fiber length of L and is constant. If the RF signal is modulated using DPSK-encoded data, the fiber-dispersion effect, which causes the fading of the photodetected RF signal, does not seriously affect the transmission quality because only two optical components, *i.e.*, one single-sideband (SSB) component and carrier, are detected. Note that

this method has the same effect as in the optical SSB-formatted transmission[2]. Third, the filtering is not performed in the optical domain but in the electrical domain to select the desired signal components. Our method will be able to provide fine and tunable filtering for the desired optical components by making good use of both the local light and the electrical BPF. This is because the frequency stability and controllability of the lasers have recently progressed in conjunction with the development of dense wavelength division multiplexing (DWDM) technologies.

2.2 Theoretical System Performance

We will now describe the SNR of the down-converted signal, $i_2(t)$, in the system using our detection method. As shown in the previous section, there was no fiber-dispersion effect in the demodulation, and therefore, we will omit the propagation constant, $\beta(f)$.

Let us rewrite the photodetected signal with no data ($\theta(t)\equiv 0$) and the local components in the real part

$$s(t) = a_s \cdot \cos\left(2\pi\left(\Delta f + f_{RF} - \frac{f_{LO}}{2}\right)t + \Delta\phi(t)\right), \quad (25)$$

$$l(t) = a_l \cdot \cos\left(2\pi\left(\Delta f + \frac{f_{LO}}{2}\right)t + \Delta\phi(t)\right), \quad (26)$$

$$a_s = \frac{1}{2}\mathcal{R}\sqrt{2P_{c1}P_{c2}}\cdot a_1, \quad (27)$$

$$a_l = \frac{1}{2}\mathcal{R}\sqrt{2P_{c1}P_{c2}}\cdot a_0. \quad (28)$$

When the shot noise is dominant, the noise spectral density, η, is given as

$$\eta = \frac{1}{4}e\mathcal{R}P_{c2}\left(1+\frac{1}{2}\frac{P_{c1}}{P_{c2}}\right). \quad (29)$$

If the input put into the multiplier is optimally bandwidth-limited, then the SNR becomes (see Appendix B)

$$\frac{S}{N} = \frac{\alpha P_{c1}}{B_{IF}}\cdot\frac{a_0^2a_1^2}{a_0^2+a_1^2}\cdot\frac{1}{2\left(1+\frac{1}{2}\frac{P_{c1}}{P_{c2}}\right)}. \quad (30)$$

Here, α [$=\mathcal{R}/e$] is the sensitivity of the PD. Under the local shot-noise limited environment ($P_{c2}\gg P_{c1}$), the SNR is given as the theoretical limit.

$$\frac{S}{N} = \frac{1}{2}\cdot\frac{\alpha P_{c1}}{B_{IF}}\cdot\frac{a_0^2a_1^2}{a_0^2+a_1^2}. \quad (31)$$

Let us consider the intensity modulation / direct detection (IM/DD) system, as shown in Fig.4[2]. The optical signal is assumed to be modulated using the same transmitter shown in Fig.1 (a). Then, the two transmitting optical signals that have no data ($\theta(t)\equiv 0$) are expressed as

$$e_{s1}(t) = \sqrt{G}E_{c1}a_1\cdot e^{j(\varphi_{c1}(t)+2\pi f_{RF}t)}, \quad (32)$$

$$e_{s0}(t) = \sqrt{G}E_{c1}a_0\cdot e^{j\varphi_{c1}(t)}, \quad (33)$$

where G is the gain of an optical amplifier with a spontaneous emission coeffcient of n_{sp}[7]. Using the square-law detection, the photodetected signal, $i_3(t)$, appears at f_{RF}. The photocurrent is expressed as

$$i_3(t) = 2\mathcal{R}GP_{c1}a_0a_1\cdot e^{j2\pi f_{RF}t}. \quad (34)$$

By downconverting with a mm-wave mixer and mm-wave local oscillator of f_{LO}, the desired signal, $i_2(t)$, which is the same signal as that given in Eq. (23), appears. If the downconverter is assumed to be ideal, the SNR of $i_2(t)$ for the conventional system becomes (see Appendix C)

$$\frac{S}{N} = \frac{\alpha P_{c1}}{B_{IF}}\cdot\frac{a_0^2a_1^2}{a_0^2+a_1^2}\cdot\frac{1}{2n_{sp}\left(1-\frac{1}{G}\right)}. \quad (35)$$

If the gain in the optical amplifier is large enough to suppress the other noise components ($G\gg 1$), then the theoretical limit of SNR is given as

$$\frac{S}{N} = \frac{1}{2n_{sp}}\cdot\frac{\alpha P_{c1}}{B_{IF}}\cdot\frac{a_0^2a_1^2}{a_0^2+a_1^2}. \quad (36)$$

Comparing Eqs. (31) and (36), we can see that the SNR for our method is improved by the amount of n_{sp}. Note that n_{sp} represents the ASE noise, which is accumulated in the link and fatally affects system performance.

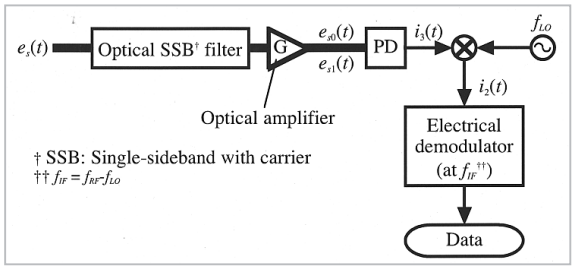

Fig.4 *Conventional IM/DD system*

3 Experiment

3.1 Experimental Setup

To verify the principle of our method, we conducted an experiment using the following setup. As shown in Fig.5, the optical system in the setup consisted of a distributed feedback laser diode (LD_1), 60-GHz-band electroabsorption modulator (EAM)[2], 3-dB optical coupler, tunable laser diode (LD_2), $LiNO_3$ modulator (EOM), erbium-doped fiber amplifuer (EDFA), optical isolator, PD, and two polarization controllers (PCs). The PNC based on the electrical square-law detector consists of two electrical amplifiers and an electric mixer (the bandwidth of the RF, LO, and IF ports were 5–18 GHz, 5–18 GHz, and DC–3 GHz, respectively).

An optical carrier (f_{c1}) was intensity modulated using a 59.6-GHz signal (f_{RF}) by the EAM. The mm-wave signal was DPSK-encoded at the data rate of 155.52 Mb/s (PRBS = $2^{23}-1$). An optical local tone (f_{c2}) and the optical signal were combined via the 3-dB coupler and optically heterodyne-detected by the PD. The tone was modulated using a 28.5-GHz [=$f_{LO}/2$] sinusoidal wave at the DC bias of V_π, which enables the suppression of the optical carrier. The EDFA was used only to amplify the optical local tone. The optically heterodyne-detected signal was amplified in the PNC by the first electric amplifier with the bandwidth of DC–26.5 GHz, was power-divided, put in the electric mixer, and amplified again by the following amplifier (2–4 GHz). The 2.6-GHz [= f_{IF}] IF signal obtained after mixing was demodulated by a DPSK demodulator to extract the data and the clock.

3.2 Experimental Results

The measured optical spectrum is shown in Fig.6. The thick and thin lines represent the optical signal and the dual-mode local tone in front of the PD, respectively. The wavelengths of LD_1 and LD_2 were 1550.27 nm [= c/f_{c1}] and 1550.17 nm [= c/f_{c2}], respectively. The optical-insertion losses of the EAM at a bias of −1.5 V and the EOM at a bias of 1.5 V were 11 and 25 dB, respectively. The

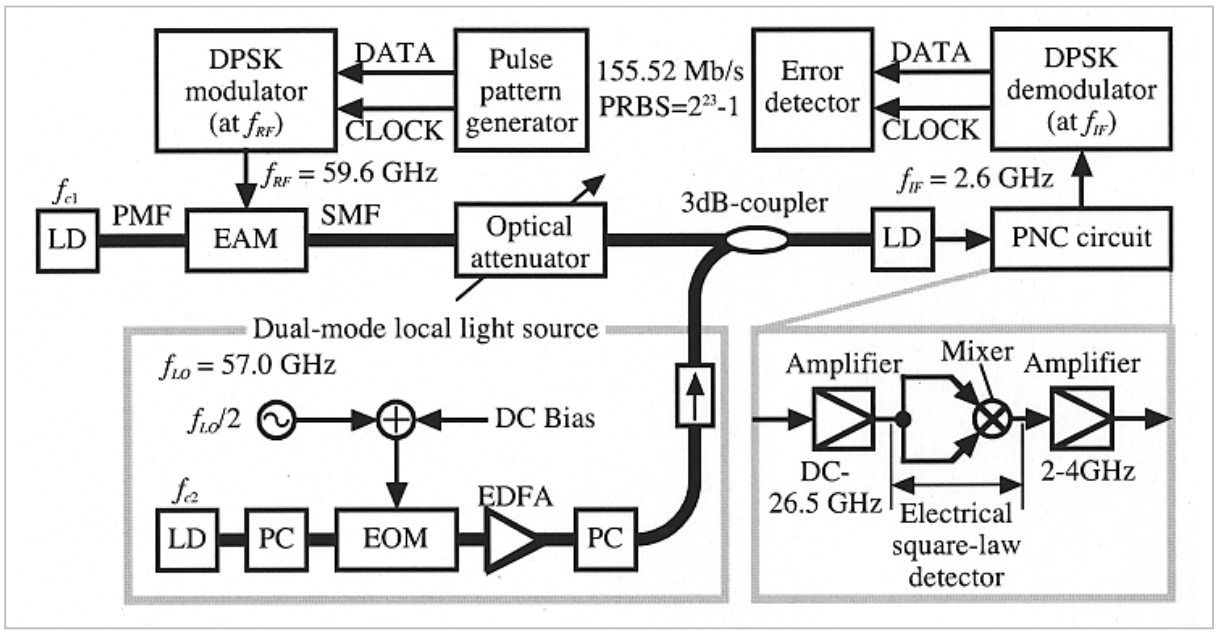

Fig.5 *Experimental setup*

power of f_{RF} applied to the EAM was 6 dBm at the same bias, corresponding to a modulation depth of about 44 %. In the optical local tone, the carrier still remained but could be removed using the present allocation of f_{c1} and f_{c2}, as shown in Fig.3.

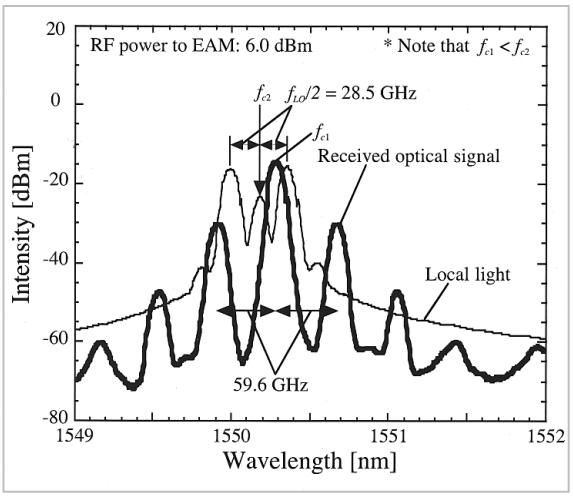

Fig.6 *Measured optical spectrum*

The photodetected signals before and after mixing were also measured. In Fig.7, the photodetected signals appear at around 12.4 GHz [$=\Delta f + f_{LO}/2$], 15.0 GHz [$=\Delta f + f_{RF} - fLO/2$], and 16.2 GHz [$=-\Delta f$]. Note that $f_{c1} < f_{c2}$. Large phase noises caused by the individually driven LD_1 and LD_2 were observed from the measured linewidths because the interval frequency between LD_1 and LD_2 were not controlled. As shown in Fig.7(b), however, a 2.6-GHz IF signal was stably generated. The observed linewidth was less than 30 Hz, and the measured SSB phase noise was less than −73 dBc/Hz at 10 kHz apart from the carrier, despite the linewidths of LD_1 and LD_2 being 5 MHz and 100 kHz, respectively. Hence, we successfully demonstrated the phase-noise cancellation.

We also measured the BERs as a function of the optical signal power put into the PD. Fig.8 (a) shows the BERs after the 25-km-long SMF transmission and the BERs for the back-to-back, which are plotted as a function of the optical signal power received by the PD. Optical local power put into the PD was −10.0 dBm. RF input power put into EAM

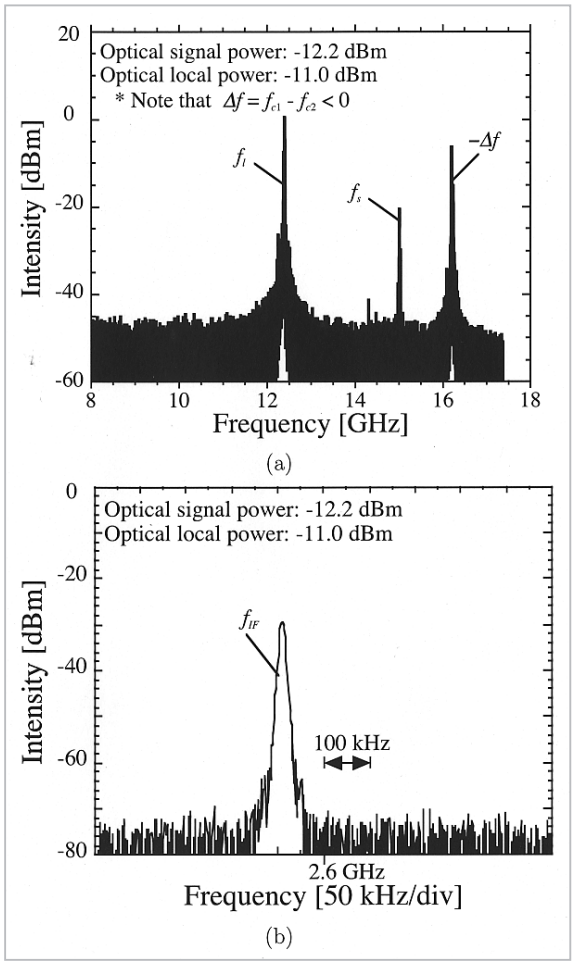

Fig.7 *Photodetected signals (a) before the mixer and (b) after the mixer*

of f_{RF} was 6.3 dBm. No BER floor was observed. The minimum optical signal power that was received to get the BER of 10^{-9} was −16.0 dBm. Compared with the back-to-back case, the small power penalty was presumably due to the polarization matching error. When the RF power was below 5.5 dBm, the BER floor appeared. This was due to the ASE noise from the EDFA that boosted the optical local tone. However the appearance of the BER floor can never pose a serious problem because it can be circumvented by using ether a 2-mode DBR-MLLD[11] or a 2-mode injection-locked FP-LD[12] as the dual-mode local light source. Fig.8 (b) shows the BERs as a function of the RF power into the EAM after the 25-km-long SMF transmission and for the back-to-back. The optical received power put into the PD was fixed to be −16.0 dBm. The BER floor did not appear. The

minimum RF input power to get the BER of 10^{-9} after the 25-km-long SMF transmission was also 6.3 dBm. Compared with the back-to-back case, no serious power penalty was observed.

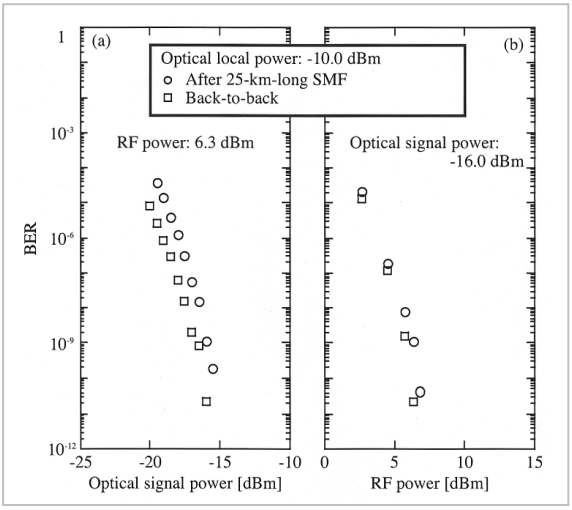

Fig.8 *BER: (a) vs. optical signal power and (b) vs. RF power*

4 Conclusion

A novel mothod for optical heterodyne detection in 60-GHz-band radio-on- fiber systems has been described. The key to detection was to photodetect the radio-on-fiber signal by using a dual-mode local light source at the receiver side. The principle and mathematical description for the detection moethod has been theoretically described. The free-running dual-mode local light was used to detect a radio-on-fiber signal at a 60-GHz band . When the photodetected signal and reference components multiplied each other, the same amount of the laser phase noise in the components were differentially subtracted. Therefore, our method was in principle free from the laser phase noise. This scheme was theoretically immune from the fiberdispersion effect, which causes signal fading because only two components of the optical signal are selected out by the local light to demodulate themselves. This immunity persisted even if the transmitted optical signal was in the DSB format. The theoretical limit of the system performance has also been derived. Compared with the conventional IM/DD system using optical amplifiers, we clarified that the proposed detection scheme is superior to the conventional one. To confirm the principle of the proposed scheme, the 25-km-long fiber-optic transmission and the optical heterodyne detection of a 59.6-GHz, 155.52-Mb/s DPSK radio-on-fiber signal has been successfully demonstrated. No serious laser phase noise and fiber-dispersion effects were occurred.

References

1 K. Kitayama, "Architectural considerations of fiber-radio millimeterwave wireless access systems," Fiber and Integrated Optics, Vol. 19, pp. 167–186, 2000.

2 T. Kuri, K. Kitayama, A. Stöhr, and Y. Ogawa, "Fiber-optic millimeterwave downlink system using 60 GHz-band external modulation," J. Lightwave Technol., Vol. 17, No. 5, pp. 799-806, May 1999.

3 T. Kuri, K. Kitayama, and Y. Ogawa, "Fiber-optic millimeter-wave uplink system incorporating remotely fed 60-GHz-band optical pilot tone," IEEE Trans. Microwave Theory and Tech., Vol. 47, No. 7, pp. 1332-1337, July 1999.

4 T. Okoshi, K. Emura, K. Kikuchi, and R. Th. Kersten, "Computation of bit-error-rate of various heterodyne and coherent-type optical communications schemes," J. Opt. Commun., Vol. 2, No. 3, pp. 89–96, Sep. 1981.

5 D. Novak, Z. Ahmed, G. H. Smith, and H. F. Liu, "Techniques for millimeter-wave optical fiber transmission systems (invited)," in Topical Meeting on Microwave Photonics (MWP'97) Tech. Dig., Duisbrug, Germany, TH1-3, Sep. 1997, pp. 39–42.

6 R.-P. Braun, G. Grosskopf, D. Rohde, and F. Schmidt, "Fiber optic millimeter-wave generation and

bandwidth efficient data transmission for broadband mobile 18–20 and 60 GHz-band communications," in Topical Meeting on Microwave Photonics (MWP'97) Technol. Dig., Duisbrug, Germany, FR2-5, pp. 235–238, Sep. 1997.

7 G. P. Agrawal, Nonlinear optics, Second Edition, Secs. 2 to 4, Academic Press, 1995.

8 M. Suzuki, Y. Noda, and Y. Kushiro, "Characterization of a dynamic spectral width of an InGaAsP/InP electroabsorption light modulator," Trans. IEICE, Vol. E69, No. 4, pp. 395–398, Apr. 1986.

9 R. M. Gagliardi and S. Karp, Optical communications, Second Edition, Sec. 1, John Wiley & Sons, Inc., 1995.

10 R. Gross, R. Olshansky, and M. Shumidt, "Coherent FM-SCM system using DFB lasers and a phase noise cancelling circuit," IEEE Photon. Technol. Lett., Vol. 2, No. 1, pp. 66–68, Jan. 1988.

11 T. Ohno, S. Fukushima, Y. Doi, Y. Muramoto, and Y. Matsuoka, "Application of uni-travelling-carrier waveguide photodiode in base stations of a millimeter-wave fiber-radio system," in Tech. Dig. MWP'99, Melbourne, Australia, F-10.2, pp. 253–256, Nov. 1999.

12 M. Ogusu, K. Inagaki, and Y. Mizuguchi, "60 GHz-band millimeterwave generation and ASK data transmission using 2-mode injectionlocking of a Fabry-Perot slave laser," in Tech. Dig. TSMMW2000, Yokosuka, Japan, P-12, pp. 181–184, Mar. 2000.

13 K. Shimoda, H. Takahashi, and C. H. Townes, "Fluctuation in amplification of quanta with application to maser amplifiers," J. Phys. Soc. Japan, Vol. 12, No. 6, pp. 686–700, June 1957.

14 H. Ishio, K. Nakagawa, M. Nakazawa, K. Aida, and K. Hagimoto, Optical amplifier and its applications, Sec. 2, Ohm, 1992 (in Japanese).

15 S. Betti, G. D. Marchis, and E. Iannone, Coherent optical communications systems, Sec. 4, John Wiley & Sons, 1995.

appendix

A Intensity Modulator

If the intensity modulation is performed, then MOD[$e_{RF}(t)$] is expressed as[8]

$$\begin{aligned}\mathrm{MOD}\,[e_{RF}(t)] &= \left[\frac{1}{2}\{1+m_{IM}\cdot\cos\varphi_{RF}(t)\}\right]^{\gamma} \\ &= \sum_{n=-\infty}^{\infty} a_n e^{jn\phi_{RF}(t)}, \end{aligned} \tag{A1}$$

where m_{IF} is the intensity-modulation index as a function of V_{RF}, and γ represents the intensity modulation with the chirp effect, which is defined as

$$\gamma = \frac{1+j\alpha_c}{2}. \tag{A2}$$

α_c is the chirp parameter of the optical modulator. We carried out the Fourier expansion of MOD[$e_{RF}(t)$] by using the Binominal theorem. As a result, we got a_n, expressed as

$$a_{\pm n} = \frac{1}{2^{\gamma}}\sum_{s=0}^{\infty}\frac{\Gamma(\gamma+1)}{(s+n)!s!\Gamma(\gamma-2s-n+1)}\cdot\left(\frac{m_{IF}}{2}\right)^{2s+n}, \tag{A3}$$

where $\Gamma(\bullet)$ is the Gamma function, which has the following relationship.

$$\Gamma(z+1) = z\cdot\Gamma(z) \tag{A4}$$

If the chirp is negligible ($\alpha = 0$), then a_n is simplified to

$$a_{\pm n} = \sqrt{\frac{1}{2}}\left[(-1)^{n-1}\sum_{l=0}^{\infty} m_{IM}^{2l+n}\cdot\frac{(2\cdot(2l+n)-3)!!}{4^{2l+n}\cdot l!(l+n)!}\right], \tag{A5}$$

where $(2n+1)!! \equiv 1\bullet 3\cdots(2n+1)$, $(2n)!! \equiv 2\bullet 4\cdots(2n)$, $0!! \equiv (-1)!! \equiv 1$, and $(-2n-1)!! \equiv (-1)^n/(2n-1)!!$. Here, we used the following formula for the natural number of n.

$$\Gamma\left(n+\frac{1}{2}\right) = \frac{(2n-1)!!\sqrt{\pi}}{2^n} \tag{A6}$$

If m_{IF} is small, then the Fourier coefficients are approximately given by

$$a_0 \simeq \sqrt{\frac{1}{2}}\left[1-\left(\frac{m_{IM}}{4}\right)^2\right], \tag{A7}$$

$$a_{\pm n} \simeq (-1)^{n-1}\sqrt{\frac{1}{2}}\frac{(2n-3)!!}{n!}\left(\frac{m_{IM}}{4}\right)^n \quad \text{for } n\neq 0. \tag{A8}$$

To verify the above calculation, we also compared $\alpha_{\pm n}$ for $m_{IF} = 1$ with the following analytical solution.

$$\sqrt{1+\cos\phi_{RF}(t)} = \sum_{n=-\infty}^{\infty}\hat{a}_n\cdot e^{jn\phi_{RF}(t)} \tag{A9}$$

$$\hat{a}_{\pm n} = \frac{2\sqrt{2}}{\pi}\frac{(-1)^{n-1}}{4n^2-1}. \tag{A10}$$

As a result, a_n numerically agreed well with the analytical solution, $\hat{a}_n$.

B SNR for Proposed Detection Technique

The photodetected signal and local components are represented by Eqs. (25) to (28). The noise spectral density at the output of the PD, η, is generally written as

$$\eta = \frac{1}{4}\left[e\mathcal{R}\left(\frac{P_{c1}}{2}+P_{c2}\right)+eI_D+\frac{2kT}{R_L}\right], \tag{A11}$$

where $\mathcal{R}$ [$= e\bullet\alpha$] is the responsivity of the photodetector. The responsibity is assumed to be the white noise, which in order, consists of the shot noises for the signal and the local light, the dark current of the photodetector (I_D), and the thermal noise ($2k_BT/R_L$). For the thermal noise, k_B, T, and R_L are the Boltzmann constant, the temperature, and the load resistance, respectively. When the shot noise is dominant, the noise spectral density, η, is approximated as

$$\eta \simeq \frac{1}{4}e\mathcal{R}P_{c2}\left(1+\frac{1}{2}\frac{P_{c1}}{P_{c2}}\right). \tag{A12}$$

$s(t)$, $l(t)$, and $n(t)$ are assumed to be statistically independent of each other, and their averages are all zero. For the square-law detector in PNC_1, the self-correlation becomes

$$
\begin{aligned}
&\mathrm{E}\left[\{s(t+\tau)+l(t+\tau)+n(t+\tau)\}^2\right. \\
&\qquad \left.\cdot\{s(t)+l(t)+n(t)\}^2\right] \\
&= R_{s^2,s^2}(\tau)+2R_{s,s}(0)\cdot R_{l,l}(0)+R_{l^2,l^2}(\tau) \\
&\quad +2\{R_{s,s}(0)+R_{l,l}(0)\}\cdot R_{n,n}(0)+R_{n^2,n^2}(\tau) \\
&\quad +4R_{s,s}(\tau)\cdot R_{l,l}(\tau) \\
&\quad +4\{R_{s,s}(\tau)+R_{l,l}(\tau)\}\cdot R_{n,n}(\tau) \qquad \text{(A13)}
\end{aligned}
$$

Here, E [•] represents the ensemble average, and $R_{x,y}(\tau)$ is the correlation function of $x(t+\tau)$ and $y(t)$ and is defined as

$$
R_{x,y}(\tau) = \mathrm{E}[x(t+\tau)\cdot y(t)]. \qquad \text{(A14)}
$$

$R_{n^2,n^2}(\tau)$ is neglected because it is much smaller than $4\{R_{s,s}(\tau)+R_{l,l}(\tau)\}\cdot R_{n,n}(\tau)$. In this case, our interest terms are the down-converted component, $4R_{s,s}(\tau)\cdot R_{l,l}(\tau)$, and the noise components, $4\{R_{s,s}(\tau)+R_{l,l}(\tau)\}\cdot R_{n,n}(\tau)$. They become

$$
\begin{aligned}
&R_{s,s}(\tau)\cdot R_{l,l}(\tau) \\
&= \frac{1}{2}\left(\frac{1}{2}a_s a_l\right)^2\cdot[\cos(2\pi f_{IF}\tau) \\
&\qquad +\cos(2\pi(2\Delta f+f_{RF})\tau \\
&\qquad\quad +2(\Delta\phi(t+\tau)-\Delta\phi(t)))], \qquad \text{(A15)} \\
&\{R_{s,s}(\tau)+R_{l,l}(\tau)\}\cdot R_{n,n}(\tau) \\
&= \frac{1}{2}(a_s^2+a_l^2)\cdot\eta\cdot\delta(\tau), \qquad \text{(A16)}
\end{aligned}
$$

where $\delta(\bullet)$ represents the delta function. From the above calculation, under the shot-noise limited environment, the SNR for the proposed detection becomes

$$
\begin{aligned}
\frac{S}{N} &\simeq \frac{4\cdot\frac{1}{2}\left(\frac{1}{2}a_s a_l\right)^2}{4\cdot\frac{1}{2}(a_s^2+a_l^2)\,\eta\cdot 2B_{IF}} \\
&= \frac{\alpha P_{c1}}{B_{IF}}\cdot\frac{a_0^2a_1^2}{a_0^2+a_1^2}\cdot\frac{1}{4\left(1+\frac{1}{2}\frac{P_{c1}}{P_{c2}}\right)}, \qquad \text{(A17)}
\end{aligned}
$$

where B_{IF} is the bandwidth of BPF_{12}. If the input put into the multiplier is optimally bandwidth-limited, then the noise power is halved. Therefore, the SNR is rewritten as

$$
\frac{S}{N} = \frac{\alpha P_{c1}}{B_{IF}}\cdot\frac{a_0^2a_1^2}{a_0^2+a_1^2}\cdot\frac{1}{2\left(1+\frac{1}{2}\frac{P_{c1}}{P_{c2}}\right)}. \qquad \text{(A18)}
$$

Under the local shot-noise limited environment ($P_{c2}\gg P_{c1}$), moreover, the theoretical limit of SNR is expressed as

$$
\frac{S}{N} \le \frac{1}{2}\cdot\frac{\alpha P_{c1}}{B_{IF}}\cdot\frac{a_0^2a_1^2}{a_0^2+a_1^2}. \qquad \text{(A19)}
$$

In the same manner, the SNR for PNC_2 is derived and acquires the same result as the above SNR.

C SNR for IM/DD

Two transmitting optical signals are assumed to have no data ($\theta(t)\equiv 0$) and expressed using Eqs. (32) and (33), respectively. In this case, because the photocurrent is given by Eq. (34), the signal power, P_s, becomes

$$
\begin{aligned}
P_s &= \frac{1}{2}|i_3(t)|^2\cdot R_L \\
&= 2(\mathcal{R}GP_{c1}a_0a_1)^2\cdot R_L. \qquad \text{(A20)}
\end{aligned}
$$

Here, G is the gain of an optical amplifier with a noise figure of n_{sp}, and R_L is the load resistance. On the other hand, the noise from the photodetector is expressed as[13][14][15]

$$
\begin{aligned}
P_n &= \left[e\mathcal{R}GP_{c1}(a_0^2+a_1^2)\right. \\
&\quad +eI_D+e^2\eta_q(G-1)n_{sp}m_t\Delta f \\
&\quad +2eG(G-1)n_{sp}\mathcal{R}P_{c1}(a_0^2+a_1^2) \\
&\quad \left.+e^2\eta_q(G-1)^2n_{sp}^2m_t\Delta f+\frac{2kT}{R_L}\right] \\
&\quad \cdot 2B_{IF}R_L \qquad \text{(A21)}
\end{aligned}
$$

In the above equation, the components are in order the shot noise for the signal and local, the dark current, the amplified spontaneous emission (ASE) shot noise, the (*signal*+*local*) $\times$*ASE* term, the *ASE*$\times$*ASE* term, and the relative intensity noise (RIN), respectively. When the signal and local shot noises are dominant, P_n is approximated as

$$
\begin{aligned}
P_n &\simeq 2eG(G-1)n_{sp}\mathcal{R}P_{c1}(a_0^2+a_1^2) \\
&\quad \cdot 2B_{IF}R_L. \qquad \text{(A22)}
\end{aligned}
$$

From the above, the SNR for the conventional IM/DD is approximated as

$$\begin{aligned}\frac{S}{N} &= \frac{P_s}{P_n} \\ &\simeq \frac{\alpha P_{c1}}{B_{IF}} \cdot \frac{a_0^2 a_1^2}{a_0^2 + a_1^2} \\ &\quad \cdot \frac{1}{2n_{sp}\left(1 - \frac{1}{G}\right)}. \end{aligned} \tag{A23}$$

If the gain of the optical amplifier is large enough to suppress the other noise components ($G \gg 1$), then the theoretical limit of SNR is given as

$$\frac{S}{N} \leq \frac{1}{2n_{sp}} \cdot \frac{\alpha P_{c1}}{B_{IF}} \cdot \frac{a_0^2 a_1^2}{a_0^2 + a_1^2}. \tag{A24}$$

***Toshiaki KURI**, Ph. D.*

Senior Researcher, Optoelectronics Group, Basic and Advanced Research Division

Optical communication systems

***Ken-ichi KITAYAMA**, Dr. Eng.*

Professor, Department of Electronic and Information Systems, Osaka University

Photonic network